

Polarization and band offsets of stacking faults in AlN and GaN

J. A. Majewski¹ and P. Vogl¹

¹Walter Schottky Institut, Technische Universität München,

(Received Saturday, July 25, 1998; accepted Tuesday, September 15, 1998)

We have performed systematic first-principles pseudopotential local density functional calculations of stacking faults in GaN and AlN. Their band offsets and the charge accumulation at stacking fault interfaces has been investigated, taking fully into account the effects of lattice relaxation and electric polarization. We find the stacking fault junctions to be of type I in both materials. However, the intrinsic valence band offsets are close to zero, so that the conduction band offsets result mostly from the differences in the energy gaps between the cubic and wurtzite phases. The charge accumulated at the interface between the cubic and wurtzite phase is found to be 0.009 and 0.003 C/m² for the AlN and GaN stacking fault, respectively.

1 Introduction

Owing to their unique material properties, III-V nitrides have a great potential for optoelectronic and high temperature, high-power microelectronic applications. A key property of the nitrides is their large spontaneous and piezoelectric internal fields [1] that allow a novel type of tailoring of the carrier dynamics and optical properties of nitride devices. One of the characteristic features of the nitrides is the large number of extended defects in these materials, which are mainly caused by the growth on lattice mismatched substrates. The influence of such defects on optical and electric properties of nitrides is not well understood up to now. However, the recent theoretical studies [2] of threading and screw dislocations in wurtzite GaN revealed that these defects are electrically inactive (i.e. without levels in the gap). Stacking faults or zinc-blende inclusions in the wurtzite matrix of AlN and GaN constitute a common type of extended defects [3] [4] [5] in these materials. In addition, it has been suggested that Mg doping can enhance the formation of zinc-blende regions. [6] Indeed, recent optical experiments suggest that the high concentration of stacking faults correlates with the presence of a deep bound exciton. [7] [8] [9]

The strong pyro- and piezoelectric character of these materials leads to a pileup of charge at the interface between two different crystallographic phases. This affects the performance of the nitride devices significantly. [10] In the present paper, we have per-

formed ab-initio calculations of zinc-blende inclusions embedded within hexagonal bulk AlN and GaN, and studied their band offsets, and the electric field resulting from the charge accumulation at the wurtzite/zinc-blende interfaces. In our calculations, the effects of lattice relaxation, and electric polarization have been fully taken into account. Additionally, we have calculated the band structure, and examined the appearance of electrically active interface gap states.

Model calculations [11] as well as first-principles calculations [12] of stacking-fault formation energies have been reported recently. The electronic structure of GaN stacking faults has been calculated in the framework of empirical pseudopotential theory. [13]

2 Stacking faults - geometry and polarization

In the wurtzite structure, the hexagonal lattice points (A, B, C) are occupied in the following stacking sequence ...ABABABAB... along the [0001] direction. In the zinc-blende structure, on the other hand, all three lattice points are occupied leading to the stacking sequence ...ABCABCABC... along the [111] direction. A stacking fault within the wurtzite structure occurs whenever the hexagonal lattice point C gets also occupied, leading to four different possible types of stacking faults (see Ref. [12]). In the present paper, we focus on the *extrinsic stacking faults* that are characterized by the following stacking sequence (AB)_n(ABC)_m and correspond to the wurtzite/zinc-blende homojunction (See Figure

1). In the present calculations, these interfaces are represented by supercells with dimension $n \leq 4$ and $m \leq 2$, respectively. We assume that all layers have the lateral lattice constant of only one phase which implies that the other one is slightly strained.

The space group $P6_3mc$ (C_{6v}^4) of wurtzite is compatible with a spontaneous polarization along the hexagonal c -axis. Therefore, the polarization can be of both pyroelectric and piezoelectric origin in the wurtzite phase, but only piezoelectric in the cubic one. Since the polarization is always parallel to the hexagonal axis, its change across the basal-plane interface is equivalent to an interface charge. The magnitude of the interface charge can be estimated from the bulk values [1] of spontaneous polarization and piezoelectric constants. In the present paper, we have determined the interface charges from self-consistent supercell calculations. These calculations show that the atomic relaxation at the interface largely influences the interface charge and the valence band offset. In fact, the relaxed interface exhibits roughly half of the charge that is associated with the unrelaxed interface.

3 Valence band offsets and interface charges

The valence band offset ΔE_V at an interface between two phases of a nitride can be conveniently split up into two terms [14]

$$\Delta E_V = \Delta \bar{V} + \Delta E_{BS}, \quad (1)$$

where $\Delta \bar{V} = \bar{V}(z_B) - \bar{V}(z_A)$ is the asymptotic difference between the laterally and vertically averaged electrostatic (Hartree plus ionic) potential $V(\mathbf{r})$ in the superlattice far from the interface (z_A and z_B denote coordinates on an axis perpendicular to the interface and lie within material A and B, respectively). The quantity $\bar{V}(z)$ is related to the macroscopically averaged electrostatic charge density $\bar{\rho}(z)$ by the Poisson equation. [14] For neutral interfaces, $\Delta \bar{V}$ equals the dipole moment of the electrostatic charge density $\bar{\rho}(z)$ across the interface. It is nonzero due to the rearrangement of the ions and electrons near the interface and therefore depends on the detailed interface geometry.

In the case of charged interfaces, the electrostatic charge density $\bar{\rho}(z)$ contains not only a dipolar contribution but also a monopole term that is proportional to the difference between the polarizations of the two materials of the heterojunction. The monopole charge density causes the macroscopically averaged electrostatic potential to change linearly with distance from

the interface rather than to approach a constant value. However, the monopole contribution to the electrostatic charge density can be filtered out [15] [16] and the intrinsic $\Delta \bar{V}$ can be obtained from the remaining dipolar contribution to $\bar{\rho}(z)$. We have calculated the charge induced at the interface σ by integrating the monopole contribution to the charge density across the interface.

The second term in Eq. (1), $\Delta E_{BS} = E_V(wz) - E_V(zb)$, is the difference between the eigenvalues of the top of the valence band in the wurtzite and zinc-blende phases of the bulk materials, measured with respect to the average electrostatic potential \bar{V} . ΔE_{BS} can be obtained from standard bulk band structure calculations for these two crystallographic phases. The spin-orbit coupling influences ΔE_{BS} and consequently the band offsets by less than 0.01 eV in the presently studied systems and may therefore be neglected. We would like to point out that in previous calculations, [13] the dipole contribution to the VBO's has been neglected.

The conduction band offset ΔE_C is defined by

$$\Delta E_C = \Delta E_V + \Delta E_{\text{gap}}, \quad (2)$$

where ΔE_{gap} is the difference between the fundamental bulk band gap in the wurtzite and zinc-blende phase of the nitride, respectively.

4 Method and computational details

The present calculations are based on the first-principles total-energy pseudopotential method within the local-density-functional formalism (LDA). [17] The LDA was implemented using the Ceperley-Alder [18] electron-gas exchange-correlation energy, as parametrized by Perdew and Zunger. [19] The Kohn-Sham equations have been solved self-consistently, employing a preconditioned conjugate gradient algorithm, [20] and minimizing the total energy with respect to the electronic density and to the ionic coordinates. The electron-ion interaction is represented by norm-conserving ionic Troullier and Martins pseudopotentials [21] cast in the separable form of Kleinman and Bylander. [22]

If one treats the semicore Ga 3d-electrons as valence electrons in the LDA calculations, one obtains much too shallow d-bands. In GaAs, for example, the calculated 3d-bands lie 3.9 eV higher than the experimental values. [23] As a result, the hybridization between Ga-3d and N-2p states gets strongly overestimated. To overcome this difficulty, we have treated the Ga 3d-states as part of the frozen core in the present calculations. The effect of the 3d-states on the valence exchange-correlation potential is properly taken into account by the so-called nonlinear core correction. [24] This procedure increases the transferability of the pseudopotentials significantly and yields lattice con-

stants, atomic positions, bulk moduli, [25] and valence band splittings of biaxially strained GaN that are in excellent agreement with experiment. [26] [27]

The presently studied supercells include up to 12 double-layers (24 atoms) along the hexagonal c axis. All atomic positions in the supercell as well as the supercell length along the c axis have been optimized by calculating the Hellmann-Feynman forces and the c -component of the stress tensor, and by preserving the hexagonal symmetry. Our calculations show that the charge induced at the wurtzite/zinc-blende interface and VBO's are insensitive to the lattice constant along c direction, but highly sensitive to the atomic relaxation at the interface (e.g. $\Delta\bar{V}$ equals 0.16 eV and 0.28 eV, respectively, for an unrelaxed and relaxed wz/zb AlN junction).

5 Results

The calculated interface charges and band offsets, together with the individual contributions as defined in Equation (1), are given in Table 1. The wz/zb interface charges and the VBO's are nearly independent on the number of wz and zb layers, provided one takes into account lattice relaxation. Since the wurtzite and zinc-blende phases are only very slightly mismatched in the basal plane (ca. 0.3 %), the computed interface charges σ and VBO's are the same irrespective of which lateral lattice constant is chosen. Consequently, only one value is given for each material in Table 1.

Our calculations predict that the band lineup of the stacking fault junction is of type I, and that the top of the valence band is marginally higher in the zinc-blende phase. The computed conduction band offsets predominantly reflect the difference in the energy gaps of the wurtzite and zinc-blende phase. We note that the conduction band offset in wz/zb AlN junction is very large which originates in the fact that the cubic phase of AlN has an indirect energy gap ($\Gamma \rightarrow X$), in contrast to the direct gap in wurtzite phase of AlN.

The large charges accumulated at the stacking fault interfaces result mainly from the spontaneous dielectric polarization of the hexagonal phase, whereas the strain-induced piezoelectric contribution is negligible. The induced charges are seen to be reduced by a factor of two by the relaxation of the atomic positions at the interface. The presently calculated charges compare well (the difference amounts to 15-20 %) with charges calculated from the statically screened bulk spontaneous polarization. [1]

The changes of the bond lengths are of the order of 0.014 Å near the wurtzite/zinc-blende interface and of order of 0.002 Å farther away from the interface. Generally, the the zinc-blende phase bond lengths adjust

themselves smoothly towards the wurtzite bond patterns. A typical relaxation pattern near a stacking fault interface is depicted in Figure 1.

As already stated above, our calculations predict that the valence band edge lies in the cubic phase for both AlN and GaN stacking faults. This originates in the dominance of the dipole contribution $\Delta\bar{V}$ to the VBO. The band structure contribution, on the other hand, causes the valence band edge to become lower in the cubic phase. This disagrees with the results of Ref. [12], where ΔE_V in GaN is equal to -0.07 eV and $\Delta\bar{V} = -0.01$ eV. Unfortunately, these small discrepancies are of the order of typical numerical errors in pseudopotential calculations, so that there remains some uncertainty as to whether the VBO is of type I or II. We note, however, that the calculations of Ref. [12] did not fully optimize the atomic positions and that our prediction seems at least not inconsistent with recent experimental data. [9]

Our calculations show that there are no interface states in the gap associated with the stacking faults. This is in accord with recent ab-initio studies, [12] but in contrast to earlier local empirical pseudopotential calculations. [13]

In Figure 2, we plot the band lineup across a cubic inclusion within a wurtzite matrix. The thin zinc-blende layer acts a dipole layer due to the divergence in the two interface polarizations. Consequently, there is a nonzero electric field within the two interfaces and a zero field outside. Experimentally, this implies that the stacking faults can generate persistent photoconductivity and they can be tuned to act either as excitonic traps or luminescence centers, depending on the width of the cubic layer.

6 Conclusions

The stacking fault homojunctions of AlN and GaN are predicted to be borderline type I with VBO's that are nearly zero, and to possess conduction band offsets that are determined by the difference in the energy gap between the cubic and the wurtzite phase. We predict no interface states to lie within the energy gap. Our calculations reveal the existence of large internal electric fields which may lead to interesting device applications.

ACKNOWLEDGMENTS

This work has been supported by the Deutsche Forschungsgemeinschaft (Project SFB 348) and the Bayerischer Forschungsverbund (FOROPTO).

REFERENCES

- [1] F. Bernardini, V. Fiorentini, D. Vanderbilt, *Phys. Rev. B* **56**, R10024 (1997).
- [2] J. Elsner, R. Jones, P. K. Sitch, V. D. Porezag, M. Elsner, Th. Frauenheim, M. I. Heggie, S. Öberg, P. R. Briddon, *Phys. Rev. Lett.* **79**, 3672 (1997).
- [3] XW Wu, LM Brown, D Kapolnek, S Keller, B Keller, SP DenBaars, JS Speck, *J. Appl. Phys.* **80**, 3228-3237 (1996).
- [4] D. Chandrasekhar, David J. Smith, S. Strite, M. E. Lin, H. Morkoc, *J. Cryst. Growth* **152**, 135-142 (1995).
- [5] Z. Liliental-Weber, C. Kisielowski, S. Ruvimov, Y. Chen, J. Washburn, I. Grzegory, M. Bockowski, J. Jun, S. Porowski, *J. Electron. Mater.* **25**, 1545 (1996).
- [6] A. Cros, R. Dimitrov, H. Angerer, O. Ambacher, M. Stutzmann, S. Christiansen, M. Albrecht, H. P. Strunk, *J. Cryst. Growth* **181**, 197 (1997).
- [7] Y. T. Rebane, Y. G. Shreter, M. Albrecht, *Phys. Stat. Sol. A* **164**, 141 (1997).
- [8] S. Fischer, G. Steude, D. M. Hofmann, F. Kurth, F. Anders, M. Topf, B. K. Meyer, F. Bertram, M. Schmidt, J. Christen, L. Eckey, J. Holst, A. Hoffmann, B. Mensching, B. Rauschenbach, *J. Cryst. Growth* **188/190**, 556 (1998).
- [9] W. Rieger, R. Dimitrov, D. Brunner, E. Rohrer, O. Ambacher, M. Stutzmann, *Phys. Rev. B* **54**, 17596 (1996).
- [10] J. A. Majewski, G. Zandler, P. Vogl, *Semicond. Sci. Technol.* **13**, 90 (1998).
- [11] A. F. Wright, *J. Appl. Phys.* **82**, 5259 (1997).
- [12] C. Stampfl, C. G. Van de Walle, *Phys. Rev. B* **57**, R15052 (1998).
- [13] Z. Z. Bandic, T. C. McGill, Z. Ikonc, *Phys. Rev. B* **56**, 3564 (1997).
- [14] A. Baldereschi, S. Baroni, R. Resta, *Phys. Rev. Lett.* **61**, 734 (1988).
- [15] J. A. Majewski, M. Stadele, *Mater. Res. Soc. Symp. Proc.* **482**, 917 (1998).
- [16] F. Bernardini, V. Fiorentini, *Phys. Rev. B* **57**, R9427 (1998).
- [17] WE Pickett, *Comp. Phys. Rep.* **9**, 115-198 (1989).
- [18] D. M. Ceperley, B. J. Alder, *Phys. Rev. Lett.* **45**, 566-569 (1980).
- [19] J. Perdew, A. Zunger, *Phys. Rev. B* **23**, 5048-5079 (1981).
- [20] MC Payne, MP Teter, DC Allan, TA Arias, JD Joannopoulos, *Rev. Mod. Phys.* **64**, 1045-1097 (1992).
- [21] N Troullier, JL Martins, *Phys. Rev. B* **43**, 1993-2006 (1991).
- [22] L Kleinman, DM Bylander, *Phys. Rev. Lett.* **48**, 1425-1428 (1982).
- [23] F. Aryasetiawan, O. Gunnarsson, *Phys. Rev. B* **54**, 17564 (1996).
- [24] SG Louie, S Froyen, ML Cohen, *Phys. Rev. B* **26**, 1738-1742 (1982).
- [25] M. Stadele, J. A. Majewski, P. Vogl, *Phys. Rev. B* **56**, 6911 (1997).

[26] J. A. Majewski, M. Städele, P. Vogl, *MRS Internet J. Nitride Semicond. Res.* **1**, 30 (1996).

[27] J. A. Majewski, M. Stadele, P. Vogl, *Mater. Res. Soc. Symp. Proc.* **449**, 887 (1997).

FIGURES

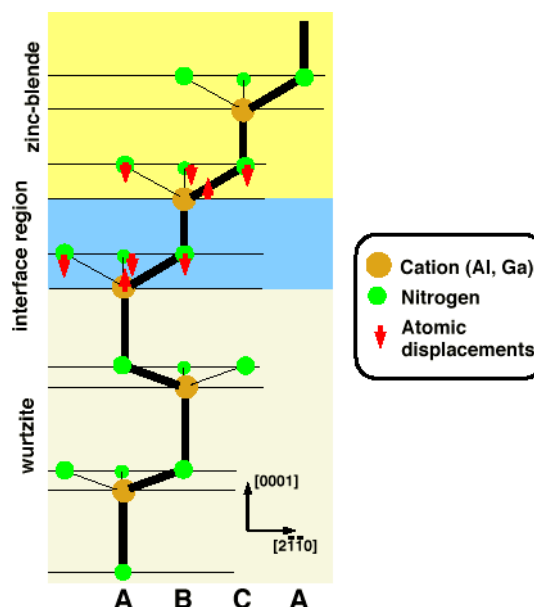


Figure 1. Schematic picture of atomic relaxation at the wurtzite/zinc-blende interface. Thick line connects atoms that lie in one plane. Note the -ABAB- stacking sequence in the wurtzite and the -ABC- sequence in the zinc-blende phase.

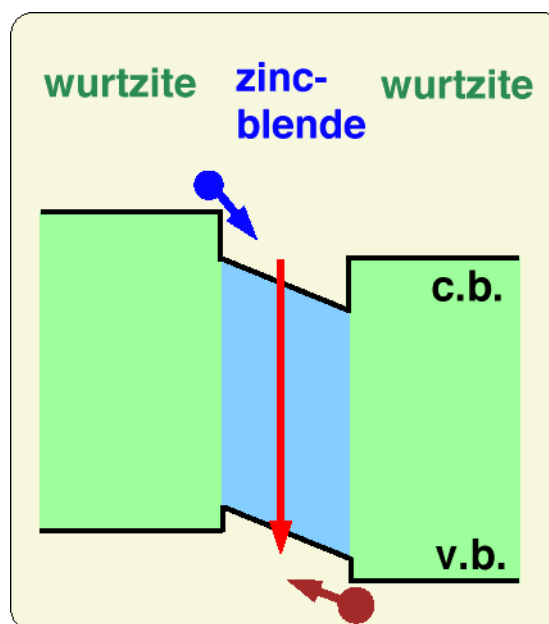


Figure 2. Band lineup of a cubic inclusion in wurtzite matrix for AlN and GaN.

TABLES

Table 1. Valence and conduction band offsets, ΔE_V and ΔE_C , potential lineups $\Delta \bar{V}$, band structure contributions ΔE_{BS} (all in eV and relative to the band edges of the wurtzite phase), and monopole interface charges σ (in C/m^2) for stacking fault interfaces. ΔE_C has been corrected by a scissor operator extracted from experimental bulk data. Values for unrelaxed interfaces are given in parenthesis. The conversion factor from C/m^2 to e/cm^2 is 6.241×10^{14} .

	AlN	GaN
ΔE_{BS}	-0.25	-0.04
$\Delta \bar{V}$	0.27 (0.15)	0.08 (0.06)
ΔE_V	0.02 (-0.10)	0.04 (0.02)
ΔE_C	1.30 (1.40)	0.12 (0.14)
σ	0.009 (0.022)	0.003 (0.006)